



## RADIOCARBON IN DISSOLVED ORGANIC CARBON BY UV OXIDATION: PROCEDURES AND BLANK CHARACTERIZATION AT NOSAMS

Li Xu<sup>1\*</sup>  • Mark L Roberts<sup>1</sup> • Kathryn L Elder<sup>1</sup>  • Mark D Kurz<sup>1,2</sup> • Ann P McNichol<sup>3</sup> • Christopher M Reddy<sup>2</sup> • Collin P Ward<sup>2</sup> • Ulrich M Hanke<sup>1,2</sup>

<sup>1</sup>NOSAMS Laboratory, Geology and Geophysics, Woods Hole Oceanographic Institution, 266 Woods Hole Road, Woods Hole, MA, 02543 USA

<sup>2</sup>Marine Chemistry and Geochemistry, Woods Hole Oceanographic Institution, 266 Woods Hole Road, Woods Hole, MA, 02543 USA

<sup>3</sup>Geology and Geophysics, Woods Hole Oceanographic Institution, 266 Woods Hole Road, Woods Hole, MA, 02543 USA

**ABSTRACT.** This study describes a procedural blank assessment of the ultraviolet photochemical oxidation (UV oxidation) method that is used to measure carbon isotopes of dissolved organic carbon (DOC) at the National Ocean Sciences Accelerator Mass Spectrometry Facility (NOSAMS). A retrospective compilation of Fm and  $\delta^{13}\text{C}$  results for secondary standards (OX-II, glycine) between 2009 and 2018 indicated that a revised blank correction was required to bring results in line with accepted values. The application of a best-fit mass-balance correction yielded a procedural blank of  $22.0 \pm 6.0 \mu\text{g C}$  with Fm of  $0.30 \pm 0.20$  and  $\delta^{13}\text{C}$  of  $-32.0 \pm 3.0\%$  for this period, which was notably higher and more variable than previously reported. Changes to the procedure, specifically elimination of higher organic carbon reagents and improved sample and reactor handling, reduced the blank to  $11.0 \pm 2.75 \mu\text{g C}$ , with Fm of  $0.14 \pm 0.10$  and  $\delta^{13}\text{C}$  of  $-31.0 \pm 5.5\%$ . A thorough determination of the entire sample processing blank is required to ensure accurate isotopic compositions of seawater DOC using the UV oxidation method. Additional efforts are needed to further reduce the procedural blank so that smaller DOC samples can be analyzed, and to increase sample throughput.

**KEYWORDS:** blank, dissolved organic carbon, radiocarbon, UV oxidation.

### I. INTRODUCTION

Dissolved organic carbon (DOC) is the largest active carbon pool in aquatic systems and is a key component of the Earth's carbon cycle (Hedges 1992). DOC is a fundamental intermediate of life in the oceans, serving as the basis of the microbial loop (Kujawinski 2011). The total amount of carbon held by DOC in the ocean is similar in magnitude to total  $\text{CO}_2$  in the atmosphere (Hedges 2002a, 2002b). DOC is operationally defined as the organic carbon that passes through a submicron filter. It is a complex mixture comprised of thousands of poorly characterized organic compounds (Kujawinski 2011). Many analytical techniques have been applied to understand compositional, spatial and temporal variability of DOC in the oceans (Hedges 2002b; Hansell et al. 2009; Moran et al. 2016), including natural abundance stable and radiocarbon isotopes ( $^{13}\text{C}$  and  $^{14}\text{C}$ ).

Stable isotope and radiocarbon measurements provide important constraints on the origin, age, and fate of oceanic DOC. For example, the age of DOC increases with depth in the ocean, similar to dissolved inorganic carbon (DIC; Williams and Druffel 1987; Druffel et al. 2019). The DOC at depth has an average age of about 6000 years, which has been attributed to the presence of numerous pools of carbon with widely differing ages (Druffel and Bauer 2000). This finding indicates that some fractions of oceanic DOC turn over rapidly, whereas other fractions persist for millennia (Follet et al. 2014). Although  $^{13}\text{C}$  and  $^{14}\text{C}$  measurements proved critical in identifying this recalcitrant marine DOC pool, the processes controlling its formation remain unknown (Hansell et al. 2009).

\*Corresponding author. Email: [lxu@whoi.edu](mailto:lxu@whoi.edu).

The method most commonly used for mineralizing seawater DOC to CO<sub>2</sub> for radiocarbon measurements is photochemical oxidation by ultraviolet light (referred to here as UV oxidation; Armstrong et al. 1966; Beupré et al. 2007). In this method, DOC is introduced to a quartz reactor, acidified, and exposed to UV radiation. The photo-produced CO<sub>2</sub> is stripped with helium gas and extracted cryogenically on a vacuum line. There are two main advantages of this method. First, given the nature of UV radiation, more than 90% of seawater DOC exposed to UV light is converted to CO<sub>2</sub>, making it an ideal mineralization technique (Armstrong et al. 1966; Beupré et al. 2007; Xue et al. 2015). Second, contamination from extraneous C is reported to be low, i.e., about 2 µg C or <1% of the DOC in 1L of seawater (Beupré et al. 2007). Based on this low blank mass, it was suggested that this method could robustly quantify the <sup>13</sup>C and <sup>14</sup>C composition of 30 mL samples of seawater DOC, representing a major technological breakthrough. However, this line blank represents only the extraneous C introduced during the UV oxidation and collection of photo-produced CO<sub>2</sub> on the vacuum line, potentially neglecting any extraneous C from the addition of acid or sample and reactor handling. There are a few laboratories capable of making the DO<sup>14</sup>C measurements using this method, and ≤2 µg C may not reflect the true magnitude of the total procedural blank in all laboratories.

DOC procedural blanks can be measured directly or indirectly. Most assessments have used the “direct method,” where acidified Milli-Q water is subjected to UV oxidation and the evolved CO<sub>2</sub> is quantified manometrically. The direct method has the advantage of providing quantitative carbon blank levels without the necessity of graphitization and accelerator mass spectrometry (AMS) measurements on small masses of carbon. An alternative blank assessment method is to perform the UV oxidation of solutions containing a series of masses of organic standards with accepted (or consensus) values for Fm and δ<sup>13</sup>C. Any deviation from the known values can be interpreted as total process blank contributions. This indirect method is more time and resource consuming because it requires isotope ratio mass spectrometry (IRMS) and AMS measurements over a range of carbon mass to allow for robust statistical blank estimates. However, the indirect method provides both an estimate of the mass and of the isotopic composition of the procedural blank C, which can in turn be used to correct samples for the procedural blank.

In this study, we compare the direct and indirect methods for assessing the procedural blanks of DOC measurements using UV oxidation. The results show that the blank determined each way agrees quite well and allowed us to investigate the potential sources of the blank. We find that the acid used for acidification and handling of the sample in the reactor is the main source of the blank. Carbon from O-rings, Milli-Q water and carrier gas play a less significant role. With the improved protocol, the procedural blank mass is reduced by 50%, from 22 µg C to 11 µg C. The new <sup>14</sup>C signature is lower with Fm = 0.14 compared to the previous value of Fm = 0.30.

## II. DOC EXTRACTION SYSTEM AND METHODS

### A. DOC Line

The NOSAMS DOC line shown in Figure 1 is custom-made and based on the system described in Beupré et al. (2007). The photochemical reactor is made from 80 mm OD, 75 mm ID UV transparent fused quartz. The top of the reactor is narrowed down to a 65/40 spherical ground glass joint, coupled with a Pyrex glass cooling probe, which cools the reactor using a dedicated recirculating water chiller at about 10 °C. The carrier gas is ultra-high purity helium (UHP, 99.999%), introduced at the center of the probe with a medium porosity glass frit at the

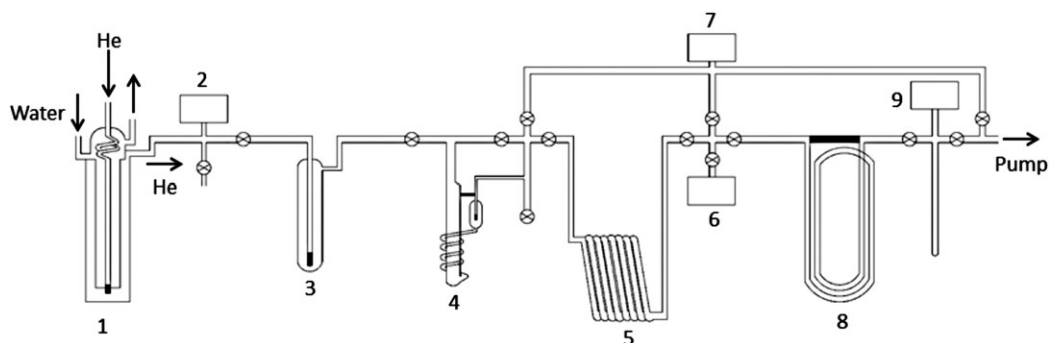


Figure 1 A schematic of the Ultraviolet Photo-oxidation and line at NOSAMS. 1.) Quartz UV oxidation reactor, 2.) 0 to 1000 torr pressure gauge, 3.) Halogen trap with acidic potassium iodide solution, 4.) Modified glass Horibe trap as water trap (in isopropyl alcohol/dry ice slush), 5.) 1/8" OD thin wall SS loop trap for CO<sub>2</sub> in LN, 6.) 0 to 1000 torr pressure gauge 7.) Thermocouple vacuum gauge for the vacuum line 8.) Glass loop water trap, 9.) Dual range MKS capacitance manometer.

bottom. The reactor is placed on top of a magnetic stirrer, with a glass encased magnet in the reactor. A 6-inch UV medium-pressure mercury arc lamp (1200 watts) is installed vertically on a frame with a parabolic reflector directed at the reactor. The assembly is placed in a continuously vented sheet metal chamber to minimize user exposure from UV light and from ozone produced by the mercury arc lamp. There are two air inlets on the side of the chamber vented with a fan through the building roof at a flow rate of 4.8 m<sup>3</sup>/min.

The main components of the system, from left to right in Figure 1, are: UV oxidation reactor, halogen trap, water trap, CO<sub>2</sub> trap and dual-range temperature-compensated MKS capacitance manometer (Model DF27 with a 5-digit voltmeter readout). Chlorine and bromine are trapped in an acidified potassium iodide solution (36 g in 70 mL Milli-Q water with 1.5 mL 85% HPLC grade phosphoric acid). Water vapor is trapped in a modified glass Horibe trap with isopropanol/dry ice slush. CO<sub>2</sub> generated from the UV oxidation of DOC is trapped in a custom 1/8" thin-wall (0.015") stainless steel tubing loop with liquid nitrogen. CO<sub>2</sub> is quantified with the capacitance manometer. The volume of the section at the manometer is 27.01 ± 0.01 cm<sup>3</sup>. The uncertainty in DOC mass quantification depends on sample size and is derived from the following equation:  $y = x \mu\text{g C} * 0.31 \% + 1.8 \mu\text{g C}$ . This uncertainty calculation comprises pressure, volume and temperature, while the 1.8 μg C corresponding to a pressure of 0.01 torr, the fluctuations caused by moisture. The main difference between this system and that described by Beaupré et al. (2007) is the stainless-steel loop used to trap the CO<sub>2</sub>, which was found to be more efficient at UHP He flow rate of 120 mL/min than a modified glass Horibe trap.

## B. Sample and Process Blank Preparation Procedures

For full volume samples, ~900 mL of sample is added to a freshly baked UV oxidation reactor (baked 5 hr at 450 °C) along with 0.5 g (equals to 16 drops from 5.25" Fisher Scientific glass pipette) of 85% phosphoric acid (HPLC grade) to acidify the sample. Prior to the summer of 2018, 1.0 g of ACS certified 85% phosphoric acid was used for acidification. The glass ball joints are sealed by carefully applying a minimum of 85% phosphoric acid (about two drops, or 0.06 g) using a freshly baked glass pipette. Subsequently, the system is purged with ultra-high purity (UHP) helium (He) at 200 mL/min for 75 min to remove dissolved

inorganic carbon (DIC). The purge time is determined by monitoring the CO<sub>2</sub> via an infrared CO<sub>2</sub> analyzer (CA-10, Sable Systems International). In the case of smaller volume samples and standards (OX-II and glycine, which are prepared from solid material with 20 to 30 g Milli-Q water in 40 mL vials, less than a few grams of solution are added to the reactor), the reactor is pre-filled with Milli-Q water (900 mL – sample volume), the cooling probe is assembled (without sealing with 85% phosphoric acid), the cooling water is connected, and the Milli-Q water is irradiated with UV for 1.5 hr. This pre-cleaning UV irradiation step reduces the potential contribution of extraneous carbon from the Milli-Q water (Griffin et al. 2010). After irradiation, the sample or standard solution (usually less than a few milliliters) is added and, after acidification, the joints are sealed with 85% phosphoric acid. DIC is then purged with UHP helium, at 200 mL/min for 75 min. DOC samples and standards are irradiated with UV for 3 hr. This UV oxidation duration was based on time series tests by Beaupre et al. (2007) and was confirmed with time series tests using our system. The generated CO<sub>2</sub> (from DOC) is purged by UHP He at 120 mL/min for 66 min, cryogenically trapped, purified, quantified manometrically, and collected by flame sealing in a 6.4 mm OD Pyrex glass tube.

Following completion of each sample, the reactor is detached from the system, and the processed sample is disposed. The cooling probe and quartz reactor are rinsed thoroughly with Milli-Q water, wrapped in aluminum foil, and baked at 450 °C in a muffle furnace overnight. This step is preventive and intended to oxidize residual organic carbon on glass surfaces that is anticipated to be the exclusive source of carbon after extensive rinsing with Milli-Q water. In this study we followed our standard protocol without further tests to evaluate the effectiveness of the glassware baking.

A test of CO<sub>2</sub> trapping efficiency of the stainless steel tube trap (Figure 1 item 5) was performed. An in-line sample cracker made of flexible stainless-steel tubing was installed between the He supply and the sheet metal chamber housing the reactor. A pre-quantified CO<sub>2</sub> sample in 6 mm OD glass tube was placed in the cracker. After a blank run, CO<sub>2</sub> collection and quantification, the sample tube was cracked, CO<sub>2</sub> was carried to the reactor at He flow of 120 mL/min and collected for 66 min. The recovered CO<sub>2</sub> was then compared to the initial sample size.

AMS measurements at NOSAMS have been described elsewhere (Roberts et al. 2010). Sample Fm measurements were made on the CFAMS system at NOSAMS (Roberts et al. 2010). Fm uncertainty for a large ( $\approx 1$  mg C) relatively modern, sample on that system is typically better than 3‰. AMS uncertainty is calculated as the larger of either the statistical uncertainty using the total number of <sup>14</sup>C counts measured for the target ( $1/\sqrt{n}$ ), or an uncertainty calculated from the reproducibility of multiple measurements of the target, both propagated with uncertainties from the normalizing standards and blank subtraction.

$\delta^{13}\text{C}$  measurements are made with a VG Optima or VG prism Isotope Ratio Mass Spectrometer (IRMS) at NOSAMS, with a typical precision in the range between 0.1‰ and 0.23‰ (e.g., Gospodinova et al. 2016; Griffith et al. 2012) for processed samples.

## **C. Blank Assessment**

### *C.1. Direct blank assessment*

About 900 mL Milli-Q water is added to the quartz reactor, similar in volume to a typical seawater DOC sample. The water cooling probe is then placed into the reactor without

sealing with 85% phosphoric acid. The Milli-Q water is exposed to UV light for 1.5 hr. Then the reactor/cooling probe is removed from the chamber. Acid (0.5 g of 85% phosphoric acid) is added to the reactor, the joints are sealed with 85% phosphoric acid. CO<sub>2</sub> is then purged with UHP helium, at 200 mL/min for 75 min. The blank is irradiated with UV for 3 hr. The generated CO<sub>2</sub> is purged with UHP helium and trapped with liquid nitrogen. It is collected in a glass flask and quantified manometrically on another dry vacuum line. Lastly, the CO<sub>2</sub> is collected and sealed in a 6.4 mm OD Pyrex glass tube.

### C.2. Indirect blank assessment using standards

Standards were used to assess the indirect blank mass and isotopic composition of the full procedural blank. OX-II and glycine standard solutions of varying carbon amounts were prepared (ranging from 0.05 to 1.0 mg C) and regularly analyzed at a ratio of two standard samples and one blank per 6 unknowns using the UV oxidation method. Since only one sample is oxidized per day, it takes a long time to accrue a meaningful number of results spanning a range of sample masses. A “mass-balance” model was then applied to these results retrospectively to determine the full sample processing blank. Modeling assumes the addition of a blank (contaminant) with a certain mass and Fm (Hanke et al. 2017; Roberts et al. 2019). In brief, the mass-balance measured Fm ( $Fm_{measured}$ ) of an unknown sample can be expressed as:

$$Fm_{measured} = \frac{Fm_{unknown} \cdot m_{unknown} + Fm_{blank} \cdot m_{blank}}{m_{unknown} + m_{blank}} \quad (1)$$

Where  $Fm_{unknown}$  and  $Fm_{blank}$  are the Fm of the unknown sample and the blank, and  $m_{unknown}$  and  $m_{blank}$  are the mass of the unknown and the blank. Solving for  $Fm_{unknown}$  gives:

$$Fm_{unknown} = \frac{Fm_{measured}(m_{unknown} + m_{blank}) - Fm_{blank} \cdot m_{blank}}{m_{unknown}} \quad (2)$$

with a corresponding uncertainty of:

$$\begin{aligned} \sigma_{Fm_{unknown}}^2 = & \left( \frac{m_{unknown} + m_{blank}}{m_{unknown}} \right)^2 \sigma_{Fm_{measured}}^2 + \left( \frac{m_{blank}}{m_{unknown}} \right)^2 \sigma_{Fm_{blank}}^2 \\ & + \left( \frac{Fm_{blank}m_{blank} - Fm_{measured}m_{blank}}{m_{unknown}} \right)^2 \sigma_{m_{unknown}}^2 + \left( \frac{Fm_{measured} - Fm_{blank}}{m_{unknown}} \right)^2 \sigma_{m_{blank}}^2 \end{aligned} \quad (3)$$

where  $\sigma_{Fm_{measured}}$ ,  $\sigma_{Fm_{blank}}$ ,  $\sigma_{m_{unknown}}$ , and  $\sigma_{m_{blank}}$  are the uncertainties in the measured Fm, blank Fm, sample mass, and blank mass respectively.

To determine the values of  $m_{blank}$  and  $Fm_{blank}$ , solutions containing known masses of OX-II and glycine were processed through the DOC system and measured on the AMS system exactly the same way as the natural samples or “unknowns”. The complete procedural blank (DOC system, graphitization and AMS) was then derived from mass balance corrections of measured data and consensus values. A total chi-squared statistic was then defined:

$$\chi^2 = \frac{1}{N} \sum_{j=1}^N \left\{ \frac{1}{n} \sum_{i=1}^n \frac{(Fm_{unknown_{ji}} - Fm_{consensus_j})^2}{\sigma_{unknown_{ji}}^2} \right\} \quad (4)$$

Where  $Fm_{consensus}$  is 1.3407 and 0.0000 respectively for OX-II and glycine,  $n$  is the number of individual measurements, and  $N$  is the number of unique sample types (in this case,

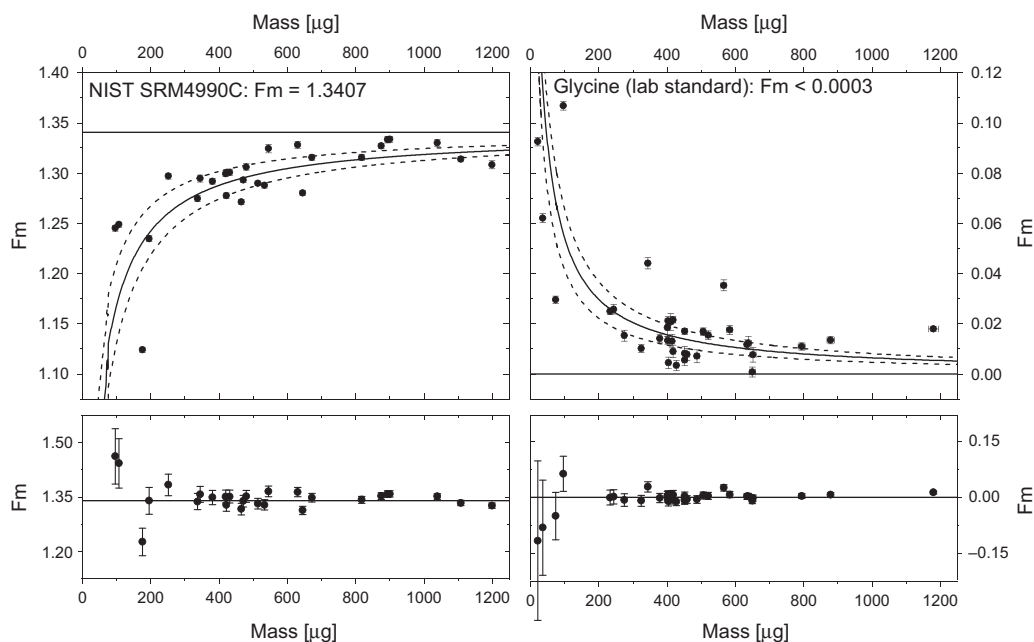


Figure 2 Compilation of  $F_m$  for two secondary standards, OX-II (left) and glycine (right), as a function of mass, during the time period 2009–2018 at NOSAMS. The horizontal lines in each diagram represent the accepted values for each material OX-II and glycine. The curves represent the estimate for impact of a blank of  $22.0 \pm 6.0 \mu\text{g C}$  with  $F_m = 0.30 \pm 0.20$ . The bottom panels show the corrected values for each determination using those blank values.

$N = 2$ ). A  $\chi^2$  statistic was initially calculated using starting values of  $m_{blank}$  and  $F_{m,blank}$ . Then, using the Solver program in Microsoft Excel (2018), the  $\chi^2$  statistic was minimized by allowing  $m_{blank}$  and  $F_{m,blank}$  to vary, subject to certain constraints (e.g.,  $m_{blank} > 0$ ,  $F_{m,blank} \leq 1$ , etc. Hanke et al. 2017; Roberts et al. 2019). This method did not allow a unique determination of the uncertainty in mass and  $F_m$  of the blank ( $m_{blank}$  and  $F_{m,blank}$ ). Therefore, we assigned an uncertainty to each such that each uncertainty contributed equally to the  $\chi^2$  statistic. For example, increasing the  $m_{blank}$  uncertainty by  $\sim 20\%$  has the same effect on the  $\chi^2$  statistic as increasing the  $F_{m,blank}$  uncertainty by 20%. The combination of the two uncertainties was also chosen such that approximately two thirds of the corrected results fall within one standard deviation of consensus values.

### III. RESULTS AND DISCUSSION

#### A. Indirect Blank Assessment: 2009–2018

Standards (OX-II and glycine) were used from 2009 to 2018 to indirectly assess the magnitude and isotopic composition of the UV oxidation procedural blank (Figure 2). Deviations from the consensus (for OX-II) or accepted (for glycine) values are assumed to be caused by procedural blank and not due to effects such as incomplete oxidation or fractionation. The best fit to the results represents a blank of  $22.0 \pm 6.0 \mu\text{g C}$  with  $F_m$  of  $0.30 \pm 0.20$ . When corrected for the magnitude and composition of the procedural blank (Figure 2 bottom panels), two thirds of the results fall within one standard deviation of the consensus or accepted values (dotted lines in Figure 2, upper panels). For OX-II ( $n = 27$ , consensus

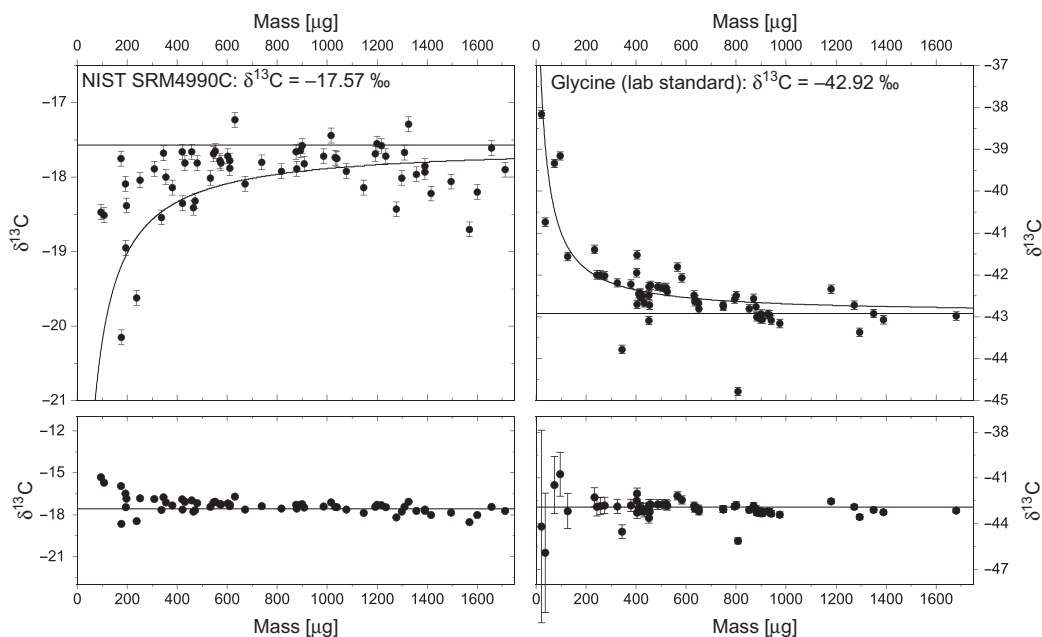


Figure 3 Compilation of  $\delta^{13}\text{C}$  for two secondary standards, OX-II (left) and glycine (right), as a function of mass, during the time period 2009–2018 at NOSAMS. The horizontal lines in each diagram represent the accepted values for OX-II and glycine. The curves represent the estimate for impact of a blank of  $22.0 \pm 6.0 \mu\text{g C}$  with  $\delta^{13}\text{C}$  of  $-32.0 \pm 3.0\text{‰}$ . The bottom panels show the corrected values for each determination using those blank values.

value 1.3407), the average Fm is  $1.350 \pm 0.020$ . The average Fm for glycine is  $0.000 \pm 0.020$  ( $n = 35$ , accepted value 0.000).

The magnitude and isotopic composition of the UV oxidation procedural blank was also determined for  $\delta^{13}\text{C}$  (Figure 3). The  $\delta^{13}\text{C}$  blank was calculated assuming the same blank mass derived from the Fm data to determine  $\delta^{13}\text{C}$  signature of the total blank over this time period. The best fit yielded an average  $\delta^{13}\text{C}$  of  $-32.0 \pm 3.0\text{‰}$  with a much larger number of individual data points for OX-II ( $n = 61$ ) and glycine ( $n = 59$ ). Uncertainties are not shown in Figure 3 because the  $\delta^{13}\text{C}$  data exceed the sample masses used to derive the mass of the blank. For the  $\delta^{13}\text{C}$  data, the corrected average value is  $-17.3 \pm 0.3\text{‰}$  for OX-II (consensus value  $-17.50\text{‰}$ ) and  $-43.0 \pm 0.5\text{‰}$  for glycine (in-house lab reference  $-42.92 \pm 0.12\text{‰}$ ;  $n = 20$  processed by closed tube combustion and elemental analysis and measured by IRMS).

The uncertainty in mass of the blank ( $m_{\text{blank}}$ ) and the isotopic composition of the blank cannot be determined independently, so we conservatively assign large uncertainties to both estimates (67% for Fm, 27% for mass). For  $^{14}\text{C}$ , the reported combined uncertainty results in approximately 68% of the blank-corrected Fm (i.e.,  $Fm_{\text{unknown}}$ ) values lying within 1-standard deviation of the consensus value (resulting in a normal distribution of results). Comparing the results of isotope data collected over the course of nine years – the measured Fm data are consistent with that of the numerical approximation yielding an adequate precision of mass ( $\pm 6.0 \mu\text{g C}$ ). The blank corrected yields account for  $95 \pm 7\%$  ( $n = 64$ ) recovery (ranging from 75% to 108%). Our test showed that efficiency of the

stainless-steel CO<sub>2</sub> trap (Figure 1 item 5) is  $100 \pm 0.5\%$  ( $n = 3$ ) for an experimental duration at 120 mL/min He flow rate for 66 min. These results suggest the stainless-steel trap can trap CO<sub>2</sub> completely. Walker et al. (2019) reported a “break through” of CO<sub>2</sub> (incomplete trapping) from glass Horibe trap.

## **B. Correction of Previously Reported Data**

The estimated procedural blank of  $22.0 \pm 6.0$   $\mu\text{g C}$  was ten-fold higher than the  $\leq 2$   $\mu\text{g C}$  previously reported (Beaupre et al. 2007). Consequently, DOC analysis at NOSAMS was suspended in the second half of 2018 in order to evaluate and improve the procedure. While efforts were undertaken to understand and reduce the DOC blank, a total of 965 DOC client analyses (including Fm,  $\delta^{13}\text{C}$  and concentration) reported between 2009 and 2018 by NOSAMS were recalculated using the determined blank and re-issued. The DOC results from this period were corrected for a total procedural blank of  $22.0 \pm 6.0$   $\mu\text{g C}$ , with an Fm of  $0.30 \pm 0.20$  and a  $\delta^{13}\text{C}$  of  $-32.0 \pm 3.0\%$  as discussed above (Table 2, 2009–2018). Between February and October 2019, reports of corrected DOC results were prepared and emailed to 56 clients. The document contained details and a spreadsheet which listed corrected DOC results with new accession numbers, together with previously reported results and sample mass for comparison. The correction increased the reported uncertainties because the final results include a complete propagation of the DOC procedural blank. The impact of this correction was largest for smaller mass (i.e.,  $<300$   $\mu\text{g C}$ ) and younger and postmodern samples. Although the corrections are generally small, they have already led to re-examination of published data from some younger samples, such as DOC in lake water (Minor et al. 2020). NOSAMS is committed to providing high quality data and the correct propagation of uncertainties.

## **C. Efforts to Lower the Blanks and to Identify Sources**

In an effort to lower the procedural blank, we took steps to minimize the introduction of extraneous C and conducted a stepwise evaluation of all potential sources of extraneous C. The potential sources included: organic residue on the reactor and cooling probe, Milli-Q water, O-rings at the helium inlet and outlet, acid for sample acidification and sealing of the glass joints, leakage of the reactor, CO<sub>2</sub> in helium (carrier gas), and handling (elimination of paper wipes, organic material from pipette bulb and glove).

The quartz reactor and Pyrex cooling probe are thoroughly rinsed with Milli-Q water three times after each experiment to minimize extraneous carbon. The reactor and cooling probe are then baked at 450 °C for 5 hr before each use, to burn off any organic residual C on the glassware.

Because the quality of the Milli-Q water can vary with time, we took measures to minimize this variability and the overall contribution of extraneous C from Milli-Q water used in the procedure. From the summer of 2018, we started to stock 4 L Milli-Q water every Monday morning when the quality is optimal, to ensure a consistent background each week. To further reduce any potential variability of DOC over time, we UV pre-treat the stocked Milli-Q water for 1.5 hr prior to each usage to minimize the blank contribution from water (except for full volume client samples which do not require additional water). Trace amounts of residual carbon even in state-of-the-art water purification systems have previously been reported, e.g., Hanke et al (2017). The UV water pre-treatment thus is



Table 1 Organic carbon levels in different mineral acids.

Acid types	Mass (g)	Method	C ( $\mu\text{g/g acid}$ )	SD
Type 1	2.0	TOC analysis	14	0.6
Type 1	4.0		8.3	0.7
Type 1	8.0		7.4	0.7
Type 1 + UV <sup>1)</sup>	8.0		2.9	0.5
Type 2	2.0		19	3.7
Type 2	4.0	UV oxidation	12	1.0
Type 2	8.0		9.0	0.7
Type 1	20.9		2.0	nd
Type 2	21.5		0.60	nd
Type 2	21.0		0.60	nd
Type 2 + UV <sup>2)</sup>	20.6		0.50	nd
Type 3 <sup>3)</sup>	19.4		0.50	nd

Note: 85% phosphoric acid (HPLC grade) Type 1 (Fisher Scientific; LOT#184413) or Type 2 (VWR; LOT# 57264816). <sup>1)</sup> 8.0 g of phosphoric acid added to 900 mL Milli-Q water, then was subject to 1.5 hr UV irradiation. <sup>2)</sup> The original acid was UV treated for 4 hr. <sup>3)</sup> Type 3: hydrochloric acid (trace metal grade; Fisher Scientific; LOT#184413). In current method, we are using 0.5 g Type 1 or Type 2, acid, or 0.4 g Type 3 acid for each run.

necessary to control for variability in water purification systems, i.e., to yield a constant level of blank carbon for isotope analyses.

Oxidized carbon from the Viton O-ring at the reactor and cooling probe can contribute to the blank. These are shielded from the lamp by the stainless-steel ultra-torr unions and the adjacent glass tubes have three glass marias to minimize UV light exposure (Beaupre et al. 2007). We shield connected glass tubes with aluminum foil to further minimize any potential impact on the blank. To test whether the Viton O-rings may be a source of blank carbon, new Viton O-rings were pre-conditioned by vacuum baking to remove any volatile carbon, i.e., to see if Viton releases any carbon during alternating heating/cooling processes. We did not observe any reduction of blank with vacuum baked O-rings (versus original ones). After the O-ring (original or vacuum baked) replacement, the first run had a higher blank, and then the blank decreased in the subsequent runs. Further, we re-exposed to UV light and collected CO<sub>2</sub> from a Milli-Q water blank (UV for 3 hr) without opening the reactor. The CO<sub>2</sub> from this second run (line blank) is usually quite small. The lowest ever line blank is 0.48  $\mu\text{g C}$  (from 0.48 to 3.8  $\mu\text{g C}$ ,  $2.3 \pm 1.3 \mu\text{g C}$ ,  $n = 10$ ). This indicates that the O-rings do not constitute a significant source for the blank carbon.

To assess the blank from phosphoric acid used in the procedure, we measured the change in DOC concentration upon addition of acid to UV treated Milli-Q water in the reactor (Table 1). Different amounts (0, 2.0, 4.0 and 8.0 g) of HPLC grade phosphoric acid Type 1 (Fisher Scientific; LOT# 184413) and Type 2 (VWR; LOT# 57264816) were added, equivalent to two, four, and eight-fold the amount used in the procedure prior to 2018. Sub samples (about 20 mL) were then submitted for an independent DOC analysis. When samples taken from the Milli-Q water system directly, the DOC concentration was  $<1 \mu\text{M C}$ . Surprisingly, adding no acid to the Milli-Q water followed by UV oxidation for three hr increased the DOC concentration to  $1.6 \pm 0.4 \mu\text{M C}$  ( $\pm 1 \text{ SD}$ ,  $n = 5$ ). Independent of the source of acid, the more acid added the higher the DOC concentration. When using Type 2

acid, the DOC concentrations in the 2.0, 4.0, and 8.0 g additions were  $3.2 \pm 0.6$ ,  $4.0 \pm 0.3$  and  $6.0 \pm 0.5 \mu\text{M C}$  ( $\pm 1$  SD,  $n = 3$ ), respectively. When using Type 1 acid, the DOC concentrations in the 2.0, 4.0, and 8.0 g additions were  $2.4 \pm 0.4$ ,  $2.8 \pm 0.2$  and  $5.0 \pm 0.3 \mu\text{M C}$  ( $\pm 1$  SD,  $n = 3$ ), respectively. Exposure of the 8.0 g Type 1 acid addition treatment to 1.5 hr of UV lowered the DOC concentration by 2.5-fold (Table 1), suggesting that the extraneous C introduced during acid addition is organic. Linear regression analyses for added acid mass and DOC allow for estimate of the contribution of C per gram acid used. The contribution of extraneous C from addition of Type 1 and Type 2 acids is  $5.4 \pm 0.4$  ( $R^2 = 0.969$ ,  $n = 3$ ) and  $5.7 \pm 0.7 \mu\text{g C}$  ( $R^2 = 0.998$ ,  $n = 3$ ).

Given that the DOC analysis indicated that C was introduced during the acid addition step in the procedure, we also employed the DOC line to assess the organic carbon loads of different acids. We added  $\sim 40$  times more acid than prescribed in the protocol, and processed it like a standard/or sample, i.e. including the UV oxidation. After pre-irradiating the Milli-Q water for 1.5 hr, approximately 20 g of acid were added to the reactor. The reactor was sealed and purged with UHP helium. After the 3-hr UV irradiation, the generated  $\text{CO}_2$  was collected and quantified using manometry. The organic carbon concentrations in the acids using this method are listed in Table 1. In general, the contribution from the acid is estimated to be less than  $1 \mu\text{g C}$  in a run, but the measurements show that carbon abundances vary with acid and supplier. This magnitude is notably lower than the TOC analysis method, perhaps because of higher power of OC oxidation using a TOC analyzer than UV oxidation. UV treatment (for 4 hr) of phosphoric acid (similar to UV pre-treatment of Milli-Q water) did not reduce the blank.

Overall, our findings indicate that the acid addition procedural step introduces extraneous C. Prior to 2018, we used 1.0 g of ACS certified 85% phosphoric acid in the procedure. In an effort to reduce the magnitude of blank C introduced during the acidification step, since 2018, we have modified the amount and purity of acid used to 0.5 g of HPLC grade phosphoric acid or 0.4 g of trace-metal grade hydrochloric acid. Moreover, the acid we use is dedicated solely for the DOC line, kept in a small bottle, and replaced every 20 runs.

Possible sources of extraneous C could be a leak in the reactor or the gas to purge off the inorganic carbon, or collection of  $\text{CO}_2$  after UV oxidation. However, methods are in place to prevent these potential sources. The reactor is leak checked after each sealing to ensure that there is no exchange with the atmosphere. This is done by adjusting helium supply pressure to atmosphere + 70 torr, closing the supply valve and watching the pressure gauge (item #2 in Figure 1) for 2–4 min, which is presumed to remain stable. The absence of  $\text{CO}_2$  contamination of the high purity helium, or leaks in the system, was also verified by “purge blanks”, which are performed after blank runs. The system is purged with helium at 120 mL/min for 66 min, with water and  $\text{CO}_2$  traps; this usually yields from 2 to 10 nanomole  $\text{CO}_2$  with an average of  $6.1 \pm 2.1$  nanomole ( $n = 17$ , post June 2018) using a smaller volume line and more sensitive pressure gauge. These results indicate that the amount of blank C from dead volumes or potential incomplete sealing of the reactor is small (i.e.,  $< 0.2 \mu\text{g C}$ ). Therefore, no changes were made to the protocol.

Additional modifications to reactor handling steps were taken in an effort to lower the magnitude of the extraneous C introduced during the UV oxidation procedure. We noticed residues on the “powder free” gloves and pipette rubber bulbs that could contribute to the blank C. Therefore, since 2018, we wash the single use gloves and bulbs with Milli-Q water

and blow dry with  $N_2$  prior to their use. We also considered the possibility that particles from paper wipes used to dry the joints of the reactor and cooling probe a source of blank C. Therefore, since 2018, we no longer use paper wipes in the procedure. Instead, we use a heat gun to dry the joints and the cooling probe. Lastly, prior to 2018 the ground glass joint of the cooling probe rested on a stainless-steel ring, which could have been a source of blank C. Therefore, since 2018, the cooling probe is held vertically by a clamp that does not directly contact the joint.

#### D. Indirect Blank Assessment Using Standards: Post 2018

Following the assessment of potential blank carbon sources, a series of standard sample measurements were carried out to indirectly quantify the new level of blank carbon in routine DOC analyses at NOSAMS. The efforts began in late 2018 and up until preparation of this manuscript, comprised OX-II ( $n = 32$ ) and glycine ( $n = 30$ ) measurements, with the results shown in Figures 4 and 5. Using the best-fit procedure described above, the modeled estimate for the procedural blank during this period is  $11.0 \pm 2.75 \mu\text{g C}$  with  $F_m$  of  $0.14 \pm 0.10$  and  $\delta^{13}\text{C}$  of  $-31.0 \pm 5.5\text{‰}$  (Figures 4 and 5). The procedural modifications described in section IIIC successfully reduced the magnitude of blank C by two-fold. While the radiocarbon data show a much better precision and accuracy for the post-2018 assessment, we observed a similar scatter in the  $^{13}\text{C}$  results demonstrating the larger variability in these data. Figure 5 left (OX-II) suggests overly narrow uncertainties (dashed lines) but this is due to the approach of assigning individual uncertainties to  $F_{m_{\text{mc}}}$  and  $\text{mass}_{\text{mc}}$  as detailed in the method section.

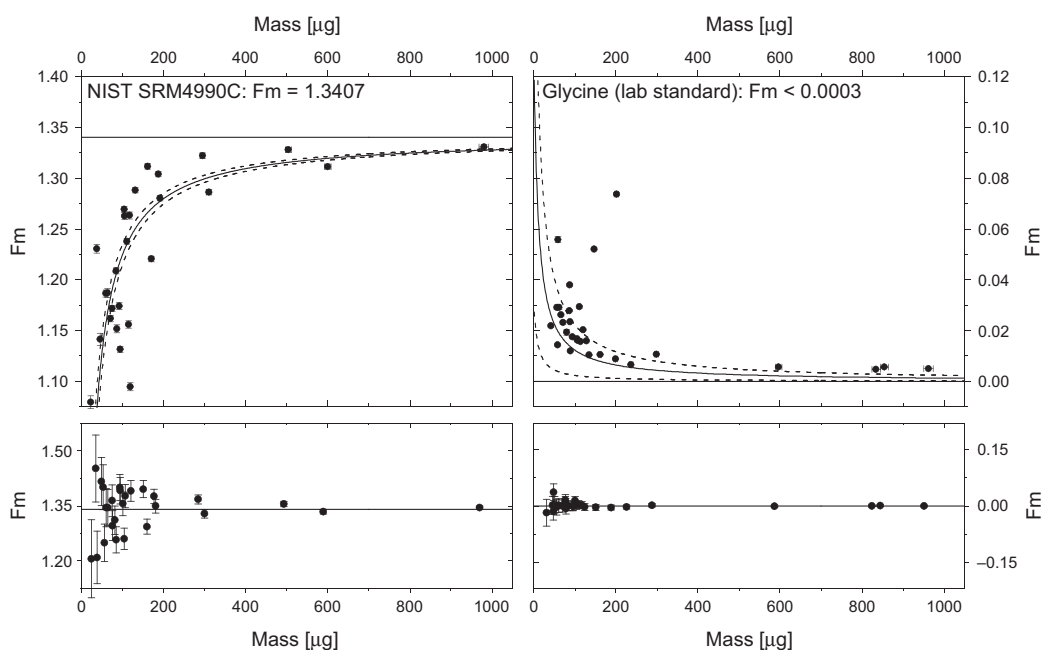


Figure 4 Compilation of  $F_m$  for two secondary standards, OX-II and glycine, as a function of mass, during the time period 2018–2019 at NOSAMS. The horizontal lines in each diagram represent the accepted values for OX-II and glycine. The curves represent the estimate for impact of a blank of  $11.0 \pm 2.75 \mu\text{g C}$  with  $F_m = 0.14 \pm 0.10$ . The bottom panels show the corrected values for each determination using those blank values.

Table 2 Mass balance blank values for DOC samples.

	Prior to 11/2018	Post-11/2018
$m_{blank}$ ( $\mu\text{g}$ )	$22.0 \pm 6.0$	$11.0 \pm 2.75$
$Fm_{blank}$	$0.30 \pm 0.20$	$0.14 \pm 0.10$
$\delta^{13}\text{C}$ (‰)	$-32.0 \pm 3.0$	$-31.0 \pm 5.5$

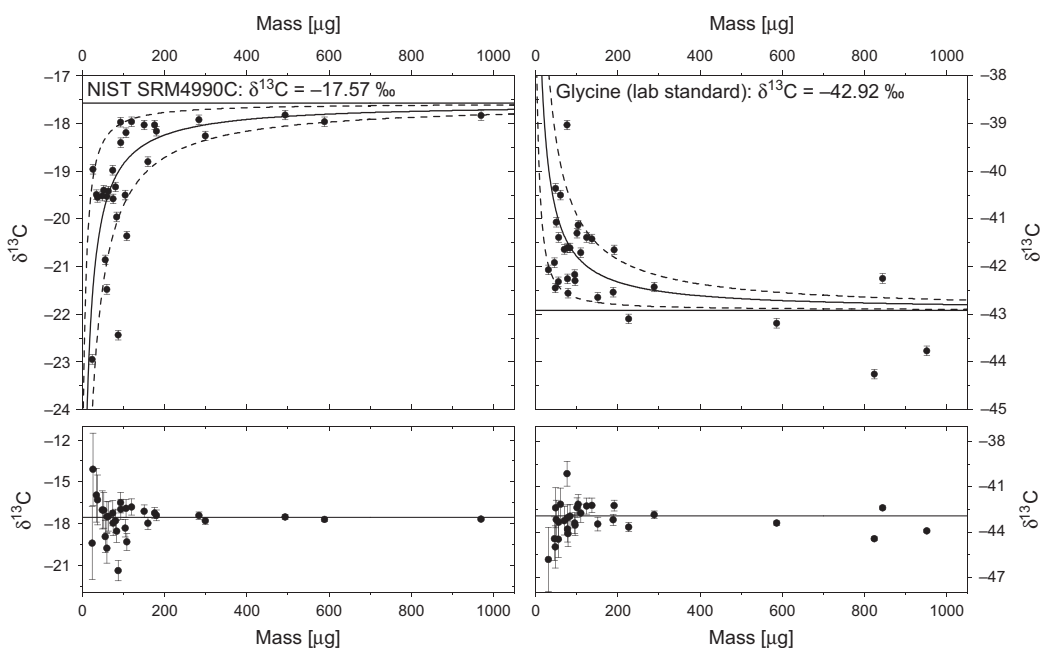


Figure 5 Compilation of  $\delta^{13}\text{C}$  for two secondary standards, OX-II (left) and glycine (right), as a function of mass, during the time period 2018–2019 at NOSAMS. The horizontal lines in each diagram represent the accepted values for OX-II and glycine. The curves represent the estimate for impact of a blank of  $11.0 \pm 2.75$   $\mu\text{g}$  C with  $\delta^{13}\text{C}$  of  $-31.0 \pm 5.5$ ‰. The bottom panels show the corrected values for each determination using those blank values.

Table 2 lists the results of both mass balance blank carbon evaluations (prior to 6/2018 and post-6/2018) showing an effective 50 % reduction in procedural blank mass and a more depleted  $^{14}\text{C}$  signature of  $Fm = 0.14$  compared to the previous value of  $Fm = 0.30$ . This depleted  $^{14}\text{C}$  signature of post-2018 blank carbon indicates a source that is dominantly of fossil origin, with only minor contributions from contemporary sources. The highly depleted  $\delta^{13}\text{C}$  data suggest the blank mass is of biological/organic origin. The difference between both blank assessments reveals a  $\delta^{13}\text{C}$  enrichment of only 1‰ in the re-assessment (post-2018 data). Note that the individual uncertainties are such that the uncertainty limits have an equal impact on chi-squared statistic. For example, using either  $m_{blank} = 13.8$   $\mu\text{g}$  with  $Fm_{blank} = 0.14$  or  $m_{blank} = 11.0$   $\mu\text{g}$  with  $Fm_{blank} = 0.24$  would give the same increase in the chi-square statistic. Regarding the efficiency of standard recovery (yields), recovery averaged  $96 \pm 8$  % ( $n = 53$ , ranging from 78% to 118%), which is similar to the recovery values in the pre-2018 data. The extreme values, for higher or lower yields, are found in measurements with small standard masses.

Table 3 Direct blank determinations (post 2018 only) by manometry, and AMS radiocarbon on combined fractions.

NOSAMS ID #	CO <sub>2</sub> quantification (μmole)			<sup>14</sup> C results	
	DOC Line	Vacuum Line	Combined	Fm	1-sigma
DOC-1819	0.30	0.300			
DOC-1851	0.32	0.270			
DOC-1857	0.33	0.273			
DOC-1865	0.54	0.540			
<b>Sample 1</b>	<b>1.49</b>	<b>1.383</b>	<b>1.34</b>	<b>0.2337</b>	<b>0.0025</b>
DOC-1869	0.70	0.654			
DOC-1895	0.25	0.227			
DOC-1905	0.49	0.478			
DOC-1914	0.36	0.358			
<b>Sample 2</b>	<b>1.80</b>	<b>1.717</b>	<b>1.71</b>	<b>0.1559</b>	<b>0.0024</b>
DOC-1923	0.63	0.640			
DOC-1932	0.65	0.647			
DOC-1941	0.63	0.611			
<b>Sample 3</b>	<b>1.91</b>	<b>1.898</b>	<b>1.87</b>	<b>0.2123</b>	<b>0.0020</b>
DOC-1950	1.11	1.140			
DOC-1959	0.47	0.482			
<b>Sample 4</b>	<b>1.58</b>	<b>1.62</b>	<b>nd</b>	<b>nd</b>	<b>nd</b>
DOC-1968	0.52	1.220			
DOC-1977	nd	0.491			
<b>Sample 5</b>	<b>0.52</b>	<b>1.711</b>	<b>1.70</b>	<b>0.2557</b>	<b>0.0020</b>

### E. Direct Blank Assessment and Comparison with Indirect Method

In addition to indirectly assessing the DOC procedural blank using secondary standards, we also conducted several direct assessments of the DOC procedural blank. During a 10-month period in 2018/2019, we carried out 14 direct blank measurements on Milli-Q water after extraction of CO<sub>2</sub> from the reactor, using manometry (Table 3). After isolation and quantification of the carbon from UV-oxidized Milli-Q water, the collected CO<sub>2</sub> was transferred and re-quantified more precisely on a smaller volume (16.43 cm<sup>3</sup>) line with a 10 torr manometer (vacuum line, see Table 3) then sealed in glass tubes. The Milli-Q water blank masses varied from 2.6 to 14.6 μg C (0.22 to 1.22 μmole CO<sub>2</sub>) with an average total C blank of 6.7 ± 3.6 μg C (0.56 ± 0.29 μmole; see Table 3). The magnitude of this blank is similar to that previously reported by Walker et al. 2019 (10 to 15 μg C for 1 L Milli-Q water) and accounts for a significant portion of the DOC procedural blank.

We combined two to four Milli-Q water blanks to yield CO<sub>2</sub> quantities that were larger than 14 μg C, to allow more reliable Fm measurements. This facilitated the successful graphitization and AMS measurement of four targets at a precision of better than 2.5‰ (Table 3). We obtained an average Fm = 0.215 ± 0.044 from the four combined direct blank tests. The same period modeled value from standards (OX-II and glycine) is 10.0 ± 2.8 μg C with Fm of 0.14 ± 0.10, indicating that the direct method and indirect method (with secondary standards) agree, within uncertainties. The product of Fm and size are also very similar (1.44 and 1.40 for the direct and indirect method, respectively). This consistency between direct and indirect blank measurements was also observed by Walker et al. (2019).

The direct blank determinations revealed variability in the manometric CO<sub>2</sub> measurements. To ensure that the sensitivity of the DOC line manometer is adequate to quantify the direct blank sample CO<sub>2</sub> yields, all isolated samples were also quantified on a second vacuum line. The results of the two different manometers are in good agreement (see the DOC and vacuum line columns in Table 3). Thus, the variability between individual manometric measurements must be due to variations in the mass of blank of the total experimental procedure, including the setup of the UV oxidation, the transfer from the reactor via vacuum line and the isolation of CO<sub>2</sub>. All experiments were carried out under the same conditions using the same acid and pre-oxidized Milli-Q water. We note that this variability in blank size is consistent with the scatter observed in the secondary standard approach and is illustrated by the scatter in Fm and δ<sup>13</sup>C illustrated in Figures 2–5 (2009–2018 and post-2018), indicating that the blank masses are variable, and may be further improved upon.

#### **F. Source Allocation of Blank Carbon at the “Current State”**

The best estimate for the DOC procedural blank mass presently at NOSAMS is  $11.0 \pm 2.75 \mu\text{g C}$ , with  $F_m = 0.14 \pm 0.10$  and  $\delta^{13}\text{C} = -31.0 \pm 5.5\text{‰}$ . This represents a two-fold improvement in the blank size for post-2018 measurements with an even more depleted blank <sup>14</sup>C signature, at almost identical δ<sup>13</sup>C values. This increases the quality of corrected data and yields a better precision. The identification of the exact causes for the remaining carbon blank is unknown, but most likely is associated with the complex analytical setup of sample transfer, reactor (with four experimental steps: loading, sealing, exposing, extracting) and the subsequent transfer through the vacuum line. Thus, we suspect that a combination of several factors led to the improvement. The most likely procedural factors appear to be (i) reducing the amount of acid used from 1 g to 0.5 g and switching to higher purity acid, (ii) extra care in covering all glassware during handling and baking, (iii) washing of gloves and pipette bulbs to eliminate adhering powder and organic residue, and (iv) elimination of paper wipe usage to dry the joints.

Isotopic signatures of the procedural blank provide important clues to potential identification of carbon sources. The DOC blank carbon is mainly <sup>14</sup>C depleted and thus most likely derived from petroleum products, such as organic solvents, Viton O-rings or other sources. Ambient air was initially considered to be a potential source of blank carbon in the sample preparation laboratories at NOSAMS due to the extensive use of dry ice and organic solvents. As a test, we measured NOSAMS laboratory air by trapping atmospheric CO<sub>2</sub> using two different vacuum lines (water stripping line (WSL) and DOC line). In both cases the sample bottle (WSL) or reactor (DOC) is filled with lab air, extracted and processed as a normal sample following the respective protocol of each line. The analyses yielded an average of  $F_m = 0.908 \pm 0.032$  and  $\delta^{13}\text{C} = -15.04 \pm 1.90\text{‰}$  ( $n = 7$ , November–December 2019). We estimated the CO<sub>2</sub> concentration in lab air to be around 1800 ppmv based on manometry, this elevated value may be caused by breathing of the lab occupants and the use of dry ice, which has an Fm of 0.893 ( $n = 1$ , February 2020). These Fm values are significantly higher than the apparent DOC blank, excluding lab air as a significant contributor. We conclude that the blank carbon is a mixture of different sources, but mostly of <sup>14</sup>C depleted organic carbon.

#### **IV. STABLE CARBON AND RADIOCARBON ISOTOPE DATA IN BLANK ASSESSMENTS**

The combination of carbon isotope data (Fm and δ<sup>13</sup>C) provide powerful means to determine the DOC procedural blanks. Both sets of isotope data can shed light on details of the blank

including the allocation of contemporary and fossil sources (Fm) and indication on types of contamination ( $\delta^{13}\text{C}$ ). For instance, from typical DIC values of about 0‰ of inorganic sources to highly depleted  $\delta^{13}\text{C}$  (organic) signatures caused by fractionation in biological processes. The impact of fractionation on the  $^{14}\text{C}/^{12}\text{C}$  ratio typically is twice that of  $^{13}\text{C}/^{12}\text{C}$ , with vast differences in natural abundance. In blank assessments of carbon isotope analyses, we trace the extraction efficiency and gas transport to compare the original sample isotope composition to that of the eventually purified sample. This comparison can be compromised by fractionation at various instances during the experiment which must be considered.

Radiocarbon is inherently more sensitive because of its larger dynamic range, and our results clearly show that  $^{14}\text{C}$  provides all information necessary to effectively troubleshoot instrumentation used to process and extract carbon for DOC isotope analyses. Another reason for the better precision of the Fm blank determination is that the data is normalized during AMS data processing to  $\delta^{13}\text{C} = -25\text{‰}$  VPDB removing the effects of isotopic fractionation. In contrast, even though the measured  $\delta^{13}\text{C}$  data are normalized to the same standard, the isotopic variations can exceed 1‰ (Figures 3 and 5) particularly at higher sample masses (above 800  $\mu\text{g C}$ ) suggesting more variability compared to radiocarbon.

$^{14}\text{C}$  measurements at natural abundance concentrations require access to AMS systems while  $\delta^{13}\text{C}$  can be measured on IRMS that are more readily available. Even though the number of accessible AMS laboratories has increased worldwide, there are also many preparative sample laboratories with custom-made extraction lines designed to submit sample materials to AMS facilities. In those laboratories, the use of  $\delta^{13}\text{C}$  (using standards) may be well suited for routine blank assessment measures. Thus, the dual isotope dataset shown here might stimulate quality assurance practices to meet the increasing high precision provided by the most recent generation of AMS systems. This study demonstrates the importance of combining samples, standards, and blanks to benchmark the overall system performance over time.

## V. RECOMMENDATIONS FOR SEAWATER DOC SAMPLES USING UV OXIDATION

The size and isotopic composition of the DOC procedural blank puts constraints on the range of environmental samples that can be analyzed at high or moderate precision using the UV oxidation method. Assuming a constant level of contamination over time, a correction of any measured sample via isotope mass balance calculation is feasible, but with the addition of uncertainties. For the current DOC blank level, the magnitudes of both data correction and uncertainty level are most drastic if the sample (Fm unknown) equals or exceeds contemporary  $^{14}\text{C}$  levels (Fm  $\sim 1$ ), due to the low Fm of the DOC blank (Fm =  $0.14 \pm 0.10$ ). The smaller the sample size, the larger the impact of the procedural blank (Figure 6). Samples that contain high, contemporary, levels of  $^{14}\text{C}$ , for instance from above ground nuclear weapon testing, are most sensitive to large differences between measured and actual sample Fm. On the other hand, “old” samples with low intrinsic Fm are quite similar to that of the blank carbon which complicates a precise determination of the actual Fm. To provide robust and meaningful data at the current state of the DOC line at NOSAMS, we recommend analyses of 900 mL samples of DOC at concentrations of 25  $\mu\text{mole}$  or higher. For samples containing less than 25  $\mu\text{mole}$ , consideration must be given to the nature of the study along with an understanding and acceptance of higher uncertainties at lower mass and higher expected Fm (Figure 6).

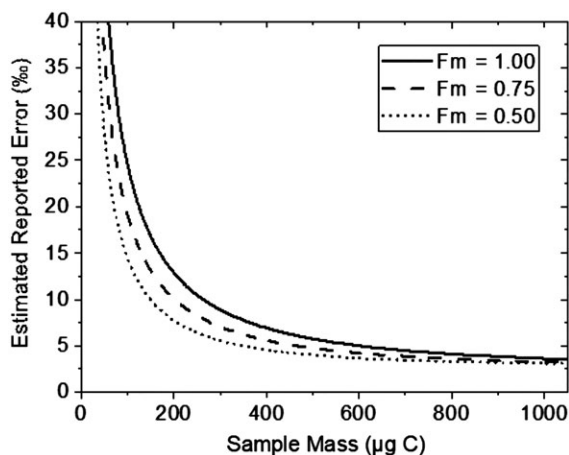


Figure 6 A plot of sample mass (x-axis) vs. estimated uncertainty on  $F_m$  (in per mil) for samples with  $F_m = 0.50$ ,  $0.75$ , and  $1.0$ , based on the post 2018 blank estimates of  $11.0 \pm 2.75 \mu\text{g C}$  with  $F_m$  of  $0.14 \pm 0.10$ .

## VI. CONCLUSION AND FUTURE PLANS

In this study we directly and indirectly assessed the magnitude and isotopic composition ( $F_m$  and  $\delta^{13}\text{C}$ ) of extraneous blank C introduced during the seawater DOC UV oxidation method, leading us to four key findings. First, a long-term (2009–2018) indirect assessment using standards resulted in a procedural blank of  $22.0 \pm 6.0 \mu\text{g C}$  with  $F_m$  of  $0.30 \pm 0.20$ ,  $\delta^{13}\text{C} -32.0 \pm 3.0\text{‰}$ . This procedural blank was an order of magnitude greater than initially estimated for the UV oxidation method (Beaupre et al. 2007). Second, using this new knowledge of the magnitude and isotopic composition of the procedural blank, NOSAMS re-analyzed and reissued results from the analysis of 965 DOC samples over a 10-year period (2009–2018). Third, we conducted a stepwise investigation into the potential sources of the blank. We concluded that low purity acid and sample and reactor vessel handling steps in the protocol were the major sources of extraneous C. Changes to the protocol based on these conclusions reduced the procedural blank by two-fold, as assessed indirectly using standards (OX-II and glycine). The UV oxidation method blank for the NOSAMS DOC sample line is currently  $11.0 \pm 2.75 \mu\text{g C}$  with  $F_m$  and  $\delta^{13}\text{C}$  values of  $0.14 \pm 0.10$  and  $-31.0 \pm 5.5\text{‰}$ , respectively. Fourth, the direct and indirect approaches to assess the magnitude and isotopic composition of the procedural blank agreed favorably (direct: mass  $6.7 \pm 3.6 \mu\text{g C}$ ,  $F_m = 0.215 \pm 0.044$ ; indirect: mass  $10.0 \pm 2.8 \mu\text{g C}$ ,  $F_m = 0.14 \pm 0.10$ , all during the same 10-month period in 2018/2019).

Collectively, these results indicate that a thorough determination of the entire procedural blank, including sample and reactor handling, the extraction line, and AMS measurements, is necessary to acquire accurate isotopic compositions of seawater DOC using the UV oxidation method.

While the analysis of seawater DOC isotopic composition over the past 50 years has substantially improved our understanding of the marine carbon cycle (Druffel and Bauer 2000; McNichol and Aluwihare 2007; Druffel et al. 2019), innovative technology is needed to address the notable limitations of the UV oxidation method. Compared to the striking



advancements in radiocarbon detection over the past 50 years (i.e., development of AMS; Burr and Jull 2009), which decreased the volume of seawater DOC required for  $^{14}\text{C}$  analysis by 200-fold (from 200 L to 1 L; Williams et al. 1969; Beaupre et al. 2007), the general approach to extract seawater DOC for isotopic analysis has not advanced much over the past decade.

These methodological limitations can be binned into two categories, the large procedural blank and low sample throughput. The procedural blank of the UV oxidation method employed for seawater DOC analysis at NOSAMS is presently 11.0  $\mu\text{g C}$  with Fm of 0.14. This procedural blank is substantially larger than for the analysis of other types of organic C: procedural blanks in compound-specific analyses on lipids (1.0  $\mu\text{g C}$ ; Shah and Pearson 2007), black carbon (3.10  $\mu\text{g C}$  and Fm of 0.435; Hanke et al. 2017), solid phase extracted marine DOC (<1.1  $\mu\text{g C/mL}$  and  $-998\%$ ; Lewis et al. 2020), freshwater DOC (0.68 to 1.05  $\mu\text{g C}$  and Fm 0.027 to 0.107; Lang et al. 2016), and bulk direct EA-IRMS-AMS analyses (6  $\mu\text{g C}$  with a Fm of 0.9; McIntyre et al. 2017). The large DOC procedural blank places limits on the versatility of the UV oxidation method, which is currently not suited to robustly analyze small volumes of seawater DOC or small fractions of the seawater DOC pool (Figure 6). The second limitation of the UV oxidation method is sample throughput. The UV oxidation procedure is labor intensive and time consuming, typically allowing processing of only one sample each day. Such low sample throughput precludes the analysis of secondary standards and blanks alongside samples, an inherent limitation of the blank evaluation described here. The low sample throughput also substantially increases analysis costs. Collectively, the large procedural blank, low sample throughput, and high costs of the UV oxidation method likely deter researchers from incorporating isotopic analysis of seawater DOC into their experiments. We anticipate that technological innovations to overcome the intrinsic limitations of the UV oxidation method will broaden the accessibility of seawater DOC isotopic measurements to the marine biogeochemistry community, leading to substantial advancements in our understanding of the marine C cycle.

## ACKNOWLEDGMENTS

This effort was supported by NSF NOSAMS cooperative agreement OCE 1755125. U.M.H. acknowledges the Swiss NSF for his postdoctoral fellowship at Woods Hole Oceanographic Institution, and the NSF for funding his Postdoctoral Investigator position at NOSAMS. Dr. Krista Longnecker provided DOC analysis with TOC analyzer. We thank Al Gagnon and Josh Burton for their assistance in the laboratory, Josh Hlanvenka for drawing Figure 1 and all other NOSAMS staff for their support. We thank the two reviewers for their helpful advice in improving this manuscript.

## REFERENCES

- Armstrong FAJ, Williams PM, Strickland JDH. 1966. Photo-oxidation of organic matter in sea water by ultra-violet radiation, analytical and other applications. *Nature* 211:481–483.
- Beaupré SR, Druffel ERM, Griffin S. 2007. A low-blank photochemical extraction system for concentration and isotopic analyses of marine dissolved organic matter. *Limnol. Oceanogr. Methods* 5:174–184.
- Burr GS, Jull AJT. 2009. Accelerator mass spectrometry for radiocarbon research. In: Gross ML, Caprioli R, editors. *Encyclopedia of Mass Spectrometry*. Vol. 5. Amsterdam: Elsevier. p. 656–669.
- Druffel ERM, Bauer JE. 2000. Radiocarbon distributions in Southern Ocean dissolved and particulate organic matter. *Geophysical Research Letters* 27:1495–1498.

- Druffel ERM, Griffin S, Wang N, Garcia NG, McNichol AP, Key RM, Walker BW. 2019. Dissolved organic radiocarbon in the central Pacific Ocean. *Geophysical Research Letters*. doi: [10.1029/2019GL083149](https://doi.org/10.1029/2019GL083149).
- Follett CL, Repeta DJ, Rothman DH, Xu L, Santinelli C. 2014. Hidden cycle of dissolved organic carbon in the deep ocean. *Proceedings of the National Academy of Sciences* 111(47): 16706-16711.
- Gospodinova K, McNichol AP, Gagnon A, Shah S. 2016. Rapid extraction of dissolved inorganic carbon from seawater and groundwater samples for radiocarbon dating. *Limol. Ocean Methods* 14:24–30. doi: [10.1002/lom3.10066](https://doi.org/10.1002/lom3.10066).
- Griffin S, Beaupr e SR, Druffel ERM. 2010. An alternate method of diluting dissolved organic carbon seawater samples for  $^{14}\text{C}$  analysis. *Radiocarbon*. 52(2):1224–1229.
- Griffith DR, McNichol AP, Xu L, McLaughlin FA, MacDonald RW, Brown KA, Eglinton TI. 2012. Carbon dynamics in the western Arctic Ocean: Insights from full-depth carbon profiles of DIC, DOC, and POC. *Biogeosciences*. 9:1217-1224. doi: [10.5194/bg-9-1217-1224](https://doi.org/10.5194/bg-9-1217-1224)
- Hanke UM, Wacker L, Haghypour N, Schmidt M, Eglinton TI, McIntyre C P. 2017. Comprehensive radiocarbon analysis of benzene polycarboxylic acids (BPCAs) derived from pyrogenic carbon in environmental samples. *Radiocarbon* 59(4):1103–1116. doi: [10.1017/RDC.2017.44](https://doi.org/10.1017/RDC.2017.44)
- Hansell DA, Carlson CA, Repeta DJ, Schlitzer R. 2009. Dissolved organic matter in the ocean: a controversy stimulates new insights. *Oceanography* 22:202–211.
- Hedges JJ. 1992. Global biogeochemical cycles: progress and problems. *Mar. Chem.* 39:67–93.
- Hedges JJ. 2002a. Sedimentary organic matter preservation and atmospheric  $\text{O}_2$  regulation. In: Gianguzza A, Pelizzetti E, Sammartano S, editors. *Chemistry of marine water and sediments*. Environmental Science. Berlin, Heidelberg: Springer.
- Hedges JJ. 2002b. Why dissolved organics matter. biogeochemistry of marine dissolved organic matter. 1-33. [10.1016/B978-012323841-2/50003-8](https://doi.org/10.1016/B978-012323841-2/50003-8).
- Kujawinski EB. 2011. The impact of microbial metabolism on marine dissolved organic matter. *Annual Review of Marine Science* 3:567–599. doi: [10.1146/annurev-marine-120308-081003](https://doi.org/10.1146/annurev-marine-120308-081003).
- Lang SQ, McIntyre CP, Bernasconi SM, Fr uh-Green G, Voss BM, Eglinton TI, Wacker L. 2016. Rapid  $^{14}\text{C}$  Analysis of Dissolved Organic Carbon in Non-Saline Waters. *Radiocarbon*. 1-11; doi: [10.1017/RDC.2016.17](https://doi.org/10.1017/RDC.2016.17)
- Lewis CB, Walker BD, Druffel ERM. 2020. Isotopic and optical heterogeneity of solid phase extracted marine dissolved organic carbon. *Marine Chemistry* 219:103752.
- McIntyre CP, Wacker L, Haghypour N, Blattmann TM, Fahrni S, Usman M, Eglinton TI, Synal HA. 2017. Online  $^{13}\text{C}$  and  $^{14}\text{C}$  Gas measurements by EA-IRMS-AMS at ETH Z urich. *Radiocarbon* 59(3):893–903.
- McNichol AP, Aluwihare L. 2007. The power of radiocarbon in biogeochemical studies of the marine carbon cycle: Insights from studies of dissolved and particulate organic carbon (DOC and POC). *Chemical Reviews* 107:443–466.
- Minor EC, McNichol AP, Zigah PK, Werne JP. 2020. Corrigendum to “An Investigation of size-fractionated organic matter from Lake Superior and a tributary stream using radiocarbon, stable isotopes, and NMR” by Zigah, P.K., Minor, E.C., Abdullah, H.A.N., Werne, J.P. and Hatcher, P.G.: A reanalysis using recent radiocarbon blank information [Geochim. Cosmochim. Acta 127 (2014) 264–284] *Geochim. Cosmochim. Acta*. 269:711–718. doi: [10.1016/j.gca.2019.11.006](https://doi.org/10.1016/j.gca.2019.11.006).
- Moran MA, Kujawinski EB, Stubbins A, Fatland R., Aluwihare LI, Buchan A, Crump BC, Dorrestein PC, Dyrhman ST, Hess NJ, et al. 2016. Deciphering ocean carbon in a changing world. *Proceedings of the National Academy of Sciences* 113(12):3143–3151. doi: [10.1073/pnas.1514645113](https://doi.org/10.1073/pnas.1514645113).
- Roberts ML, Burton J, Elder K, Longworth B, McIntyre C, von Reden K, Han B, Rosenheim B, Jenkins W, Galutschek E, et al. 2010. A high-performance  $^{14}\text{C}$  accelerator mass spectrometry system. *Radiocarbon* 52(2):228–235. doi: [10.1017/S003822200045252](https://doi.org/10.1017/S003822200045252).
- Roberts ML, Elder K, Jenkins W, Gagnon A, Xu L, Hlavenka J, Longworth B. 2019.  $^{14}\text{C}$  Blank Corrections for 25–100  $\mu\text{g}$  Samples at the National Ocean Sciences AMS Laboratory. *Radiocarbon* 61(5):1403–1411. doi: [10.1017/RDC.2019.74](https://doi.org/10.1017/RDC.2019.74).
- Shah SR, Pearson A. 2007. Ultra-microscale (5–25  $\mu\text{g}$  C) analysis of individual lipids by  $^{14}\text{C}$  AMS: Assessment and correction for sample processing blanks. *Radiocarbon* 49:69–82.
- Walker BD, Beaupr e SB, Griffin S, Druffel ERM. 2019. UV photochemical oxidation and extraction of marine dissolved organic carbon at UC Irvine: status, surprises, and methodological recommendations. *Radiocarbon* 61(5):1603–1617. doi: [10.1017/rdc.2019.9](https://doi.org/10.1017/rdc.2019.9)
- Williams PM, Oeschger H, Kinney P. 1969. Natural radiocarbon activity of dissolved organic carbon in North-East Pacific Ocean. *Nature* 224: 256–258.
- Williams PM, Druffel ERM. 1987. Radiocarbon in dissolved organic matter in the central North Pacific Ocean. *Nature* 330: 246–248.
- Xue Y, Ge T, Wang X. 2015. An effective method of UV-oxidation of dissolved organic carbon in natural waters for radiocarbon analysis by accelerator mass spectrometry. *Journal of Ocean University of China* 14:989–993.